International Journal of Hyperthermia

ISSN: 0265-6736 (Print) 1464-5157 (Online) Journal homepage: www.tandfonline.com/journals/ihyt20

Uncovering the time-temperature thresholds of *in vitro* mitochondrial bioenergetics dysfunction under hyperthermic stress

Natasha F. Mezzacappo, Natalia M. Inada, José D. Vollet-Filho, Michael L. Denton, Vladislav V. Yakovlev & Vanderlei S. Bagnato

To cite this article: Natasha F. Mezzacappo, Natalia M. Inada, José D. Vollet-Filho, Michael L. Denton, Vladislav V. Yakovlev & Vanderlei S. Bagnato (2025) Uncovering the time-temperature thresholds of *in vitro* mitochondrial bioenergetics dysfunction under hyperthermic stress, International Journal of Hyperthermia, 42:1, 2560017, DOI: 10.1080/02656736.2025.2560017

To link to this article: https://doi.org/10.1080/02656736.2025.2560017

Published online: 22 Sep 2025.

INTERNATIONAL JOURNAL OF HYPERTHERMIA
2025, VOL. 42, NO. 1, 2560017
https://doi.org/10.1080/02656736.2025.2560017

Taylor & Francis
Taylor & Francis Group

Uncovering the time-temperature thresholds of *in vitro* mitochondrial bioenergetics dysfunction under hyperthermic stress

Natasha F. Mezzacappo[a,b], Natalia M. Inada[a,b], José D. Vollet-Filho[a], Michael L. Denton[c], Vladislav V. Yakovlev[b] and Vanderlei S. Bagnato[a,b]

[a]São Carlos Institute of Physics, University of São Paulo (USP), São Paulo, Brazil; [b]Department of Biomedical Engineering, Texas A&M University, College Station, TX, USA; [c]Air Force Research Laboratory, Bioeffects Division, JBSA Fort Sam Houston, San Antonio, TX, USA

ABSTRACT

Mitochondrial respiration is particularly vulnerable to temperature fluctuations, yet time-dependent effects of hyperthermia on mitochondria remain largely unexplored. In this study, we evaluated the thermal sensitivity of mitochondria isolated from mouse liver using high-resolution respirometry (HRR) to assess the combined effects of temperature elevation and exposure time. Our results demonstrated that isolated mitochondria experienced progressive dysfunction of the electron transport chain (ETC) and the phosphorylation system as both temperature and incubation time increased. Notably, even moderate thermal stress led to significant impairments, and damage became irreversible when exceeding 40% at a minimum temperature of 43 °C. A mathematical analysis of the time-temperature relationship further supported these findings, highlighting a threshold beyond which mitochondrial function cannot recover. These results emphasize the importance of accounting for the degree of heat exposure and its duration when evaluating thermal effects on mitochondrial bioenergetics. This study provides valuable insights into mitochondrial resilience's *in vitro* thermal limits.

ARTICLE HISTORY
Received 30 May 2025
Revised 12 August 2025
Accepted 5 September 2025

KEYWORDS
Hyperthermia; mitochondria; bioenergetics; time-temperature; respirometry

1. Introduction

Body metabolism generates heat, and thermoregulation maintains temperature balance [1,2]. When heat production exceeds dissipation, core temperature rises, leading to hyperthermia or fever, conditions with similar symptoms but different physiological causes [1,2]. Hyperthermia can result from intense exercise, hot environments [3,4], or be induced therapeutically to treat tumors by increasing the local temperature in the 40–43 °C range using laser irradiation [5,6]. Cellular heat stress disturbs membrane balance [7,8], triggering adaptive and survival responses [9], such as the activation of heat shock proteins (HSPs), which protect against irreversible protein denaturation [7,8,10,11] and can reverse protein unfolding and aggregation [12]. Heat stress in the range of 39–42 °C for 15–20 min can be considered mild without significant consequences [9], while severe stress (43–45 °C) may cause membrane disruption, oxidative stress, and apoptosis. Heat-induced damage depends on both temperature and exposure time, and may involve reversible or irreversible cellular effects, including mitochondrial membrane permeability and reactive oxygen species (ROS) production [7,8,13].

Cells may activate repair mechanisms in response to heat injury, but severe damage can be irreversible. Thomsen and Pearce (2011) identified two photothermal damage levels: primary effects, causing immediate structural and functional disruption, and secondary effects, reflecting delayed cellular responses [14]. A key primary effect is the early increase in mitochondrial membrane permeability to ions [14].

CONTACT Natasha F. Mezzacappo natasha.mezz@gmail.com; natasha.mezzacappo@usp.br São Carlos Institute of Physics, University of São Paulo (USP), São Carlos, SP13566-590, Brazil

Mitochondria are the primary source of heat production in endothermic organisms, enabling them to maintain a stable body temperature regardless of environmental conditions [15]. Most of this metabolic heat is generated by the electron transport chain (ETC) and oxidative phosphorylation (OXPHOS), through proton leakage and electron transfer within the inner mitochondrial membrane [16,17]. While some studies suggest that mitochondria may be warmer than their surrounding cellular environment [17], this remains debated due to concerns about measurement methodologies [16,18,19]. Challenging the idea of higher localized mitochondrial temperatures, Moreno-Loshuertos et al. (2023), demonstrated that mitochondria undergo heat stress at temperatures above 43 °C [19]. Such stress can impair mitochondrial function by inhibiting ATP synthesis, disrupting the ETC, and triggering the opening of the mitochondrial permeability transition pore (mPTP) due to calcium overload [8]. This leads to membrane rupture and cytochrome c release, ultimately activating apoptosis via the mitochondrial pathway [8].

Although mitochondrial responses to hyperthermia have been studied from various angles [19–24], the role of exposure time—crucial for understanding thermal dose [25]—has largely been overlooked. Incubation protocols vary across studies, and duration is often not reported. In this study, we investigated time-dependent thermal effects on mitochondrial respiration *in vitro*, using mitochondria isolated from mouse liver. This model was selected to assess the direct impact of heat *in organello* [19], as isolated mitochondria offer a robust system for studying specific bioenergetic processes with greater experimental control and manipulability [26,27]. We also performed a mathematical analysis of the time–temperature relationship by generating isoeffect curves to quantify thermal damage. To our knowledge, this is the first study to examine the combined impact of temperature and exposure time on mitochondrial respiration using a mathematical approach based on *in vitro* data.

2. Materials and methods

2.1. Experimental design

To investigate time-dependent, heat-induced changes in mitochondrial respiration, we will analyze mitochondria isolated from mouse liver using the high-resolution respirometry (HRR) technique with an Oxygraph-2k respirometer (OROBOROS, Austria). As outlined in Figure 1, the samples will first be incubated under varying time and temperature conditions in a water bath. Following incubation, mitochondrial respiration will be assessed using HRR to determine the effects of thermal exposure.

2.2. Reagents

The followed chemicals used were purchased from Sigma-Aldrich (St. Louis, MO, USA): ADP (A5285), bovine serum albumin (BSA, A9418), CCCP (C2759), dibasic potassium phosphate (K_2HPO_4, P5504), EGTA (E4378), glutamic acid (G1501), HEPES (H3375), malic acid (M1000), and oligomycin A (O4876). These other chemicals were purchased from VWR® Avantor (Radnor, PA, USA): sucrose (M117), potassium chloride (KCl, 26752.366), magnesium chloride hexahydrate ($MgCl_2$, BDH9244), and potassium hydroxide (KOH, 0489). All solutions were prepared using ultrapure Milli-Q® water. The pH of all solutions was adjusted to 7.2 with potassium hydroxide (KOH).

2.3. Animals

Wild-type adult female C57BL/6J mice ($N = 5$, 8 weeks old) were purchased from The Jackson Laboratory and maintained in the Laboratory Animal Care Building (LARR). The animals were kept in ventilated rack housing containing individual air injections, under illumination in a 12:12 h light: dark cycle, with food and water *ad libitum*. The animals were acclimatized, and the experiments were performed when the animals were between 9 and 12 weeks old. All protocols in this study were approved by the Institutional Animal Care and Use Committee from Texas A&M University (IACUC 2023-0137) and followed the ethical guidelines.

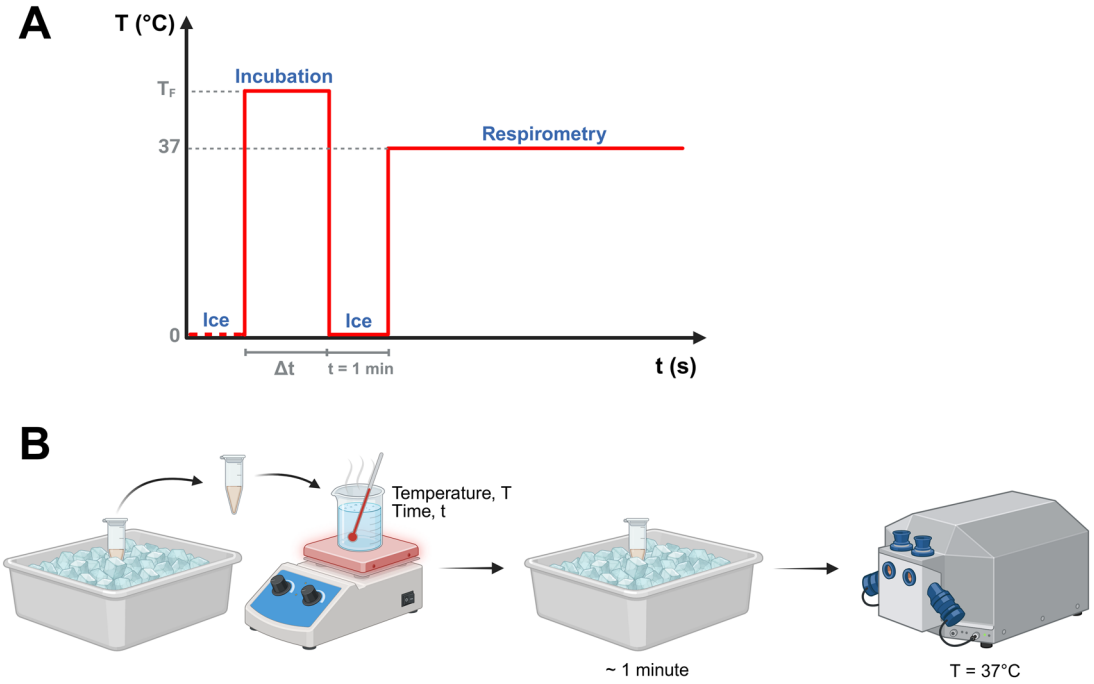

Figure 1. Experimental design of the incubation conditions and temperature variation for isolated mitochondria. Created with BioRender.com.

2.4. Isolation of mouse liver mitochondria

Immediately before the experiments, animals were euthanized by fast cervical dislocation without anesthesia [26] and death was confirmed by checking the lack of vital signs. The extraction was performed through a peritoneal incision to access and remove the liver with the aid of surgical scissors and Foerster forceps. Mitochondria were isolated using a differential centrifugation method [28]. All isolation procedures were conducted in an ice bath or at 4 °C. Briefly, the liver was rapidly excised and immediately transferred to an ice-cold isolation buffer I (250 mM sucrose, 0.5 mM EGTA, and 10 mM HEPES; pH 7.2), where it was minced with scissors in an ice bath and homogenized in a Potter-Elvehjem tissue homogenizer (Wheaton™ Overhead Stirrer, DWK Life Sciences, USA) at 300 rpm, using a glass tube and a polytetrafluoroethylene (PTFE) pistil. The resulting homogenate was transferred to a conical 50 ml plastic tube, with the volume completed to 40 ml with the isolation buffer I, and centrifuged using a benchtop refrigerated centrifuge (HIGHConic II Fixed Angle Aluminum Rotor, Thermo Scientific, USA) for 10 min at 800 × g and 4 °C. The obtained supernatant was transferred to another conical 50 ml plastic tube and centrifuged at 7700 × g and 4 °C for 10 min. Following the supernatant disposal, the resulting pellet was carefully brushed using a pony hair round brush (size 0), avoiding potential blood cell residuals, and transferred to another 50 ml plastic conical tube with 25 ml of isolation buffer II (250 mM sucrose, 0.3 mM EGTA, and 10 mM HEPES; pH 7.2) and centrifuged again for 10 min at 7700 × g and 4 °C. The final pellet containing mitochondria was carefully washed three times with isolation buffer III (250 mM sucrose and 10 mM HEPES; pH 7.2) and resuspended in an aliquot of the same buffer. The protein concentration of the isolated mitochondria was determined using the Bradford method [29] with different concentrations of BSA as standards.

2.5. Induction of temperature increase

2.5.1. Characterization of temperature increase

The increase pattern of each temperature condition was evaluated with a needle thermocouple (MT-29/1HT Needle Microprobe, Physitemp Instruments).

2.5.2. Thermal stress and respirometry of isolated mitochondria

After isolation, the mitochondria sample was aliquoted (50 µL) in microtubes and incubated in a water bath at the respective test temperature (37, 43, 45, or 47 °C) [19] for different periods (1, 5, and 10 min). The temperature variation is shown in Figure 1. After incubation, the aliquots were kept in an ice bath for approximately 1 min for thermal normalization.

Mitochondrial oxygen consumption was analyzed by HRR using the Oxygraph-2k respirometer (OROBOROS, Austria). Air calibration was performed daily before the experiments at 37 °C, with a stirrer speed of 750 rpm, in the 2 ml chambers of the Oxygraph-2k, using the standard reaction buffer defined in [28]: 125 mM sucrose, 65 mM KCl, 2 mM K_2HPO_4, 1 mM $MgCl_2$, and 10 mM HEPES (pH 7.2). The oxygen flux (negative time derivative of oxygen concentration) was corrected for instrumental background [30].

After treatment, samples were diluted to 0.5 mg/mL in the standard mitochondrial respiration buffer within the respirometer chamber. Glutamate (5 mM) and malate (2.5 mM) were used as substrates. Oxygen consumption rate (OCR) was measured at 37 °C with a stirrer speed of 750 rpm, following the SUIT (substrate-uncoupler-inhibitor titration) protocol adapted from SUIT-006 [31]: 500 µM ADP, 10 µM cytochrome C, 1 µg/mL oligomycin, and 50–250 nM CCCP stepwise titrations. The following respiratory parameters were assessed (Table 1) based on the titrations: BASAL, OXPHOS, $LEAK_{Omy}$, ET capacity, RCR, and E–L coupling efficiency (J_{E-L}).

2.6. Statistical analysis

OCR data were recorded as O2 flux normalized per mass (pmol/(s*mg)) by DatLab 7.4 (OROBOROS, Austria) and analyzed using Origin 2022 (OriginLab®, USA). To evaluate the combined effects of temperature and incubation time on mitochondrial function, data were first tested for normality using the Shapiro–Wilk test. Upon confirmation that the data followed a normal distribution, two-way ANOVA was performed, with temperature and incubation time as independent factors. Each experimental run was treated as a replicate. When a significant main effect or interaction was detected ($p \leq 0.05$), *post hoc* comparisons were conducted using Tukey's multiple comparisons test. Percentage changes for each condition were calculated relative to the control group (37 °C, 10 min incubation) using the mean values of each parameter. This percentage-based approach was adopted to facilitate direct comparisons between groups in the text and to provide an intuitive measure of the magnitude of change relative to the reference condition. Curves of temperature characterization and mathematical analysis were performed using Origin 2022 software (OriginLab®, USA).

3. Results

3.1. Characterization of temperature increase

Figure 2 illustrates the heating profiles of isolated mitochondria subjected to different final temperature conditions, with samples at an initial temperature of 1.1 ± 0.3 °C due to the storage on ice to minimize metabolic activity and preserve mitochondrial integrity. The mitochondrial suspensions (volume: 50 µL) were transferred to a water bath for controlled heating, and the temperature was recorded over time to monitor thermal transitions. Within the first ~60 s, the temperature of all samples increased rapidly and reached thermal equilibrium, demonstrating efficient heat transfer in the small-volume preparation. This

Table 1. Parameters related to the analysis of oxygen consumption (adapted from Gnaiger (2020) [31]).

Parameter	Occurrence	Meaning
$LEAK_n$ (L_n)	Mitochondria with substrates	Mitochondrial respiration without exogenous ADP
OXPHOS (P)	ADP addition	Oxidative Phosphorylation
$LEAK_{Omy}$ (L)	Oligomycin addition	Proton leak stage, when respiration is measured after exhausting OXPHOS or after inhibition of ATP synthase by oligomycin
ET capacity (E)	Uncoupler addition	Maximal respiratory capacity of ETS after uncoupling the respiration
RCR	P/L	An indicator of the mitochondria sample quality, evaluating the defects in the ETS, ATP synthase, and the variation in proton leak [32]. 'Healthy' and high-quality samples will have high respiratory control [33].
E-L coupling efficiency (J_{E-L})	J_{E-L} = (E–L)/E	Indicator of the OXPHOS capacity limitation due to the phosphorylation system capacity [31]

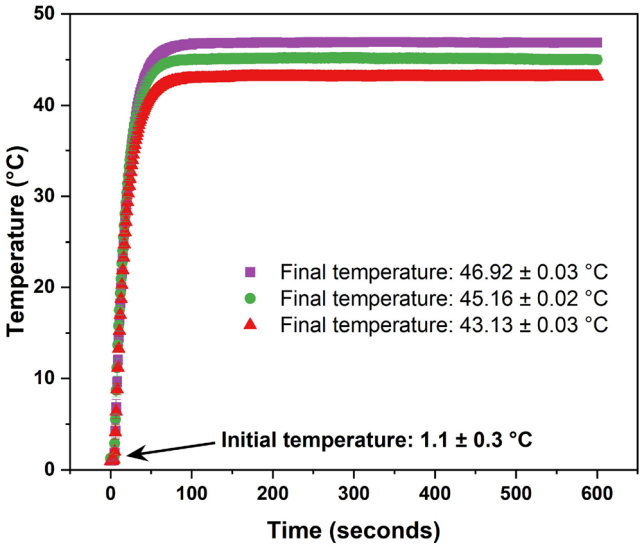

Figure 2. Heating profile relative to the isolated mitochondria in different final temperatures, with a volume of 50 µL and the sample initially maintained in ice.

heating profile validates the accuracy and reproducibility of the thermal protocol used to expose isolated mitochondria to different degrees of hyperthermia. The time to reach steady-state temperature is critical, as it defines the actual exposure duration at the target temperature.

3.2. Thermal stress of isolated mitochondria

3.2.1. Respirometry analysis

The parameters related to oxygen consumption for isolated mitochondria after thermal stress are shown in Figure 3. $LEAK_n$ OCR (Figure 3(A)) remained relatively unchanged across temperatures and incubation times ($p > 0.05$ for all comparisons). Both OXPHOS and ET capacity showed progressive reductions with increasing temperature and longer exposure times. For OXPHOS (Figure 3(B)), the decrease ranged from 38.1% (43 °C, $t = 5$ min) to 74.6% (47 °C, $t = 10$ min) compared to the control ($p = 0.0156$ and $p < 0.0001$, respectively), indicating a marked impairment in ATP-producing respiration. ET capacity (Figure 3(D)) declined in a similar pattern, with the most severe decrease (71.5%) observed at 47 °C for 10 min when compared to the control ($p < 0.0001$), demonstrating that maximum respiratory capacity was also substantially compromised under severe thermal stress. The comparable magnitude of decline in both parameters suggests that the primary site of heat-induced dysfunction lies within the electron transport chain, rather than being restricted to the phosphorylation system. Proton leak ($LEAK_{omy}$, Figure 3(C)) increased significantly, particularly at 47 °C for 10 min, reaching a 96.8% increase relative to control ($p = 0.0295$), suggesting that membrane integrity is increasingly compromised at high temperatures. These alterations led to a reduction E-L coupling efficiency (Figure 3(D)), starting to be significant at 47 °C in 5 min ($p = 0.0020$ when compared to the control), reflecting severe disruption of mitochondrial bioenergetic regulation. RCR (Figure 3(E)) also decreased markedly with both temperature and time, especially from 43 °C onward, reaching critically low values (86.6% decrease) at 47 °C for 10 min compared to control ($p < 0{,}0001$), consistent with loss of mitochondrial efficiency and respiratory coupling. At $t = 1$ min, no significant differences were observed across temperatures when compared to the control ($p > 0.05$), likely because this reflects the time required to reach stable target temperatures, as shown in Figure 2.

3.2.2. Mathematical analysis

The percentage of damage relative to the control (non-incubated sample) was calculated using RCR values (Figure 4(A)). RCR was chosen as the damage indicator because it reflects overall mitochondrial function by balancing OXPHOS and proton leak. Since any disruption in these processes directly affects RCR [33]. It serves as a reliable metric for estimating mitochondrial damage. The data points in Figure 4(A) were fitted using Equation (1):

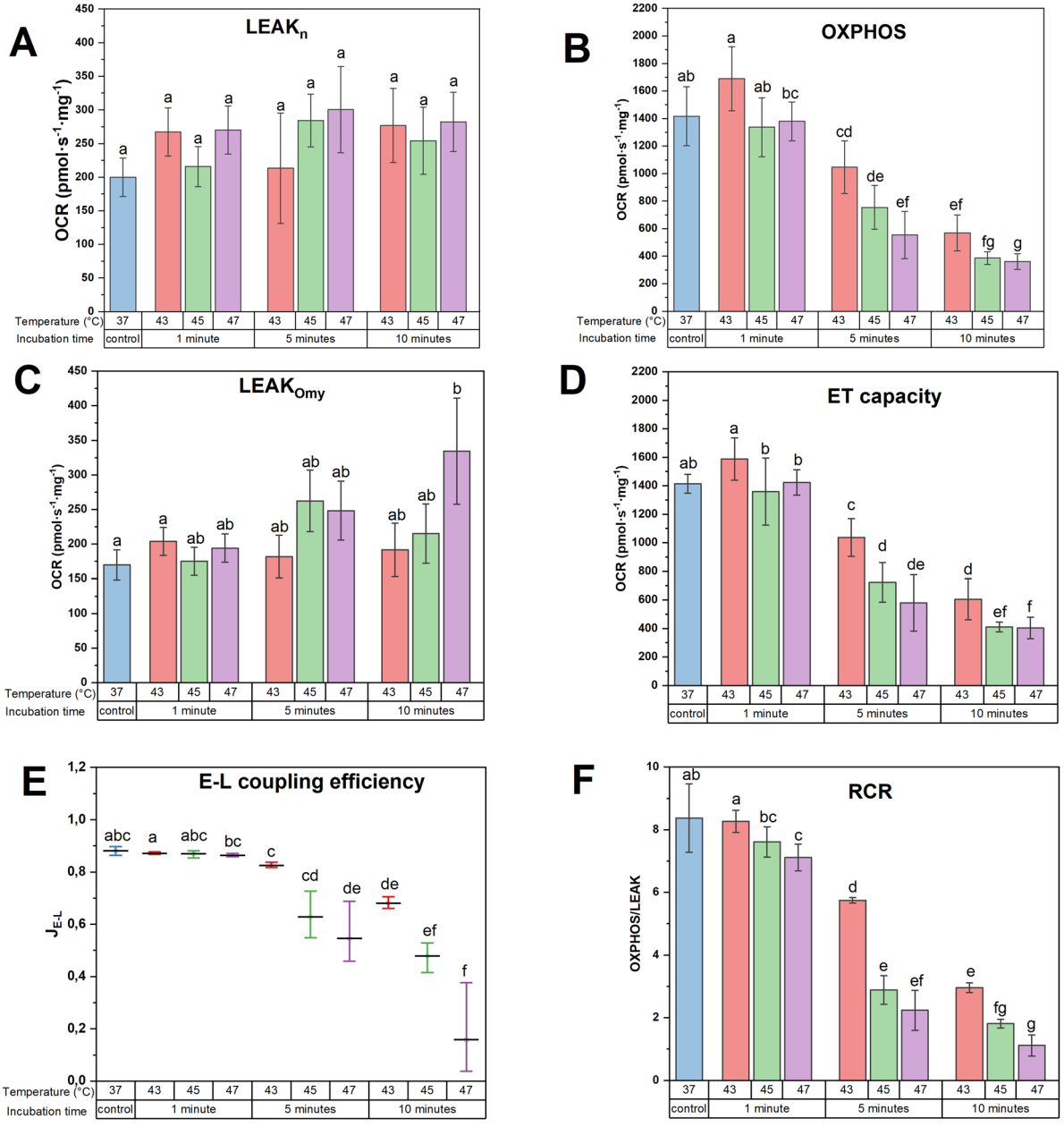

Figure 3. Parameters related to oxygen consumption after thermal stress in mitochondria isolated from mouse liver. (A) BASAL; (B) OXPHOS; (C) LEAK$_{Omy}$; (D) ET capacity; (E) E-L coupling efficiency; (F) RCR. For clarification on the meaning of each parameter, see Table 1. Control is the sample incubated at 37 °C for the longest time (10 min). Groups were compared using a two-way ANOVA ($N = 5$ animals, with 3 to 5 replicates per group), followed by Tukey *post hoc* tests. Values are mean ± standard deviation, with the letters (a, b, c, d, and e) in the groups indicating statistical significance ($p \leq 0.05$), in which groups with the same letters are not significantly different from each other.

$$D_{RCR} = e^{\left(\frac{\alpha_T}{T}\right)}\left(1 - e^{\left(\frac{-t}{\beta_T}\right)}\right) \quad (1)$$

where D_{RCR} is the damage level (from 0 to 1) related to the control using RCR values, α_T, and β_T are physical quantities calculated from the best fit to data points, T is the temperature in °C, and t is the time in seconds. The proposed expression is a variation of the Arrhenius equation [34], an empirical function to describe the chemical kinetics relation with temperature. Equation (1) was also obtained empirically, based on *in vitro* data, to associate the temperature with the exposure time. It conjugates the limitations imposed by the increase in temperature; at the same time, it shows that different effects have characteristic times to reach stationary

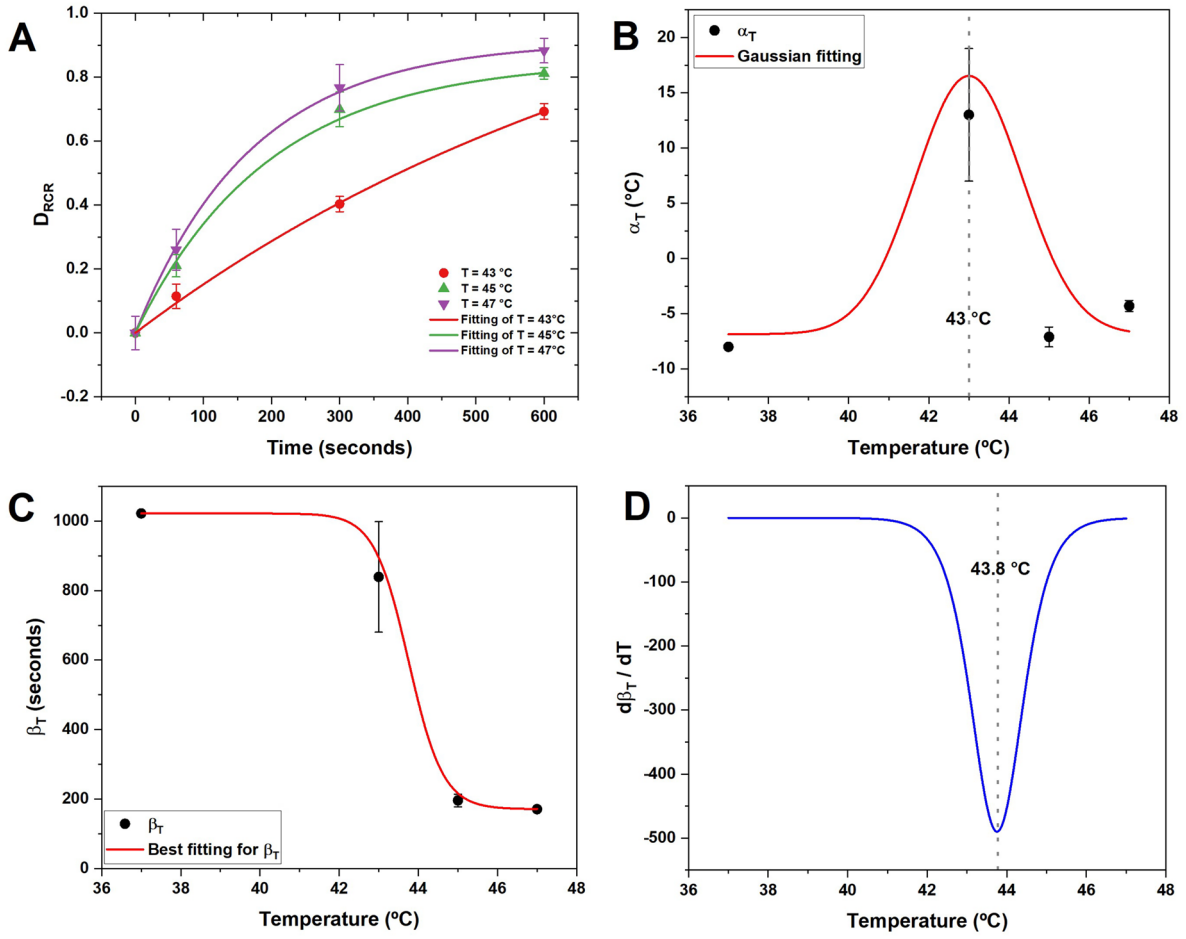

Figure 4. Mathematical analysis using RCR values. (A) Percentage of damage related to the control, calculated from RCR values (D_{RCR}), over the incubation time. Fitting curves were obtained using Equation (1). (B) Variation of α_T with the temperature, with a Gaussian fitting for the data points centered near 43 °C. (C) Variation of β_T with the temperature and the best fit for the data points. (D) Derivative of β_T fitting related to temperature, with an inflection point at 43.8 °C (dashed reference line).

Table 2. Physical quantities obtained from the fitting curves for each temperature.

Temperature (°C)	α_T (°C)	β_T (s)
43	13.0	838.6
45	−7.12	196.0
47	−4.3	171.2

states. The expression provided here serves as an empirical tool to enhance the discussion on the relationship between temperature and exposure time within the temperature range investigated in this study. The parameters α_T and β_T, respectively in units of temperature and time, allow for an assessment on how the thermal energy associated with the temperature and the rate of delivery of such energy are related and must be taken into account.

Analysis of α_T and β_T from each temperature fitting (Table 2) revealed that their values varied in response to changes in temperature. Based on this, we concluded that α_T and α_T must be temperature-dependent, with their relationship to temperature illustrated in Figure 4(B,C). For α_T, a Gaussian-like relationship can be observed among the data points, with a peak centered around 43 °C (Figure 4(B)). It is interesting to note that, for our data, there is a signal change in α_T as the temperature crosses immediately beyond 43 °C. This signal change shows that the thermal effects at both regions (immediately below and above the threshold temperature of about 43 °C) are different.

In contrast, β_T exhibits a pattern similar to logistic decay (Figure 4(C)), with the decay also starting around 43 °C. For each temperature, β_T is related to how long such a temperature can be maintained before damage is observed. The decrease in values obtained for β_T indicates that, at lower temperatures, specific temperatures can be kept for more extended periods (resulting in a higher β_T value). In contrast, beyond the threshold of approximately 43 °C, these temperatures can be sustained for significantly shorter durations before damage occurs (resulting in a lower β_T value). This decay is attributed to a significant increase in thermal damage, suggesting a shift in the importance of the temporal component at and beyond this temperature. Analyzing the derivative of the function estimated for β_T points (Figure 4(D)), we identified an inflection point centered around 43.8 °C, emphasizing the transition between the levels of mitochondrial damage. The intrinsic meaning of the derivative function allows us to confirm the change in the heating profile at this point.

Analysis of β_T suggests a shift between two distinct modes of thermal damage, divided by a critical temperature of 43 °C, supported by the same threshold observed for the change in the signal of α_T, and thus of the first exponential behavior beyond 43 °C, which then leads to an increasing damage rate over time. Below this threshold, damage follows a gradual mechanism, where mitochondrial function is preserved mainly due to the balance between damage and active repair processes, thus requiring more prolonged exposure to produce noticeable impairment. Above 43 °C, a more rapid damage mechanism predominates. This shift is consistent with the idea that repair mechanisms become overwhelmed, leading to protein unfolding and denaturation [14], which, under our experimental conditions, was not reversed during the subsequent respirometry measurements. The decay shown in Figure 4(C) mirrors the characteristic pattern of protein unfolding under thermal stress [35,36], supporting this interpretation. Consequently, damage progresses quickly beyond this temperature and becomes apparent even after brief exposure times.

Isoeffect curves were derived from Figure 5(A) by fixing specific damage levels, resulting in the time-versus-temperature plots shown in Figure 5(B). From the curves in Figure 5(A), it appears that damage plateaus around 40%, indicating a saturation point. Based on these observations, we propose that when damage exceeds 40% at temperatures above 43 °C, a threshold is crossed beyond which functional recovery was not observed within the time frame of our *in vitro* assays (highlighted as the gray region in Figure 5(B)). We interpret this as a potential point of no return under our experimental conditions, where damage progresses rapidly and repair processes are no longer sufficient to restore measurable mitochondrial function.

4. Discussion

The *in vitro* hyperthermia parameters selected for this study were inspired mainly by the work of Moreno-Loshuertos et al. (2023) [19], who addressed whether mitochondria could achieve local temperatures higher than the surrounding cellular environment [16,18]. Although this was not the primary focus of our investigation, our findings may contribute valuable insight to that ongoing discussion. As previously stated, our study centered on the relationship between thermally induced mitochondrial damage and incubation time.

While basal respiration remained largely unaffected, OXPHOS and ET capacity declined to a similar extent, indicating that the primary limitation under hyperthermic conditions lies within the ETC itself. The concomitant increase in proton leak further suggests that loss of membrane integrity contributes to the observed dysfunction, compounding the reduction in ATP-producing respiration. These findings are consistent with earlier research by Christiansen and Kvamme (1969) who reported membrane damage in mouse brain and liver mitochondria following a 10-min heat exposure at temperatures up to 45 °C [37]. The unaffected BASAL agrees with the results from Žūkienė et al. (2017) [22], who studied isolated liver mitochondria exposed to temperatures ranging from 37 to 52 °C. Although some studies have reported increased basal respiration under heat stress [20], but Žūkienė et al. (2017) proposed that such findings may stem from methodological differences, particularly the use of real-time respiration measurements at elevated temperatures, rather than post-incubation assessments. This distinction suggests that previously observed increases in basal respiration may represent transient and reversible responses to acute heat exposure [22].

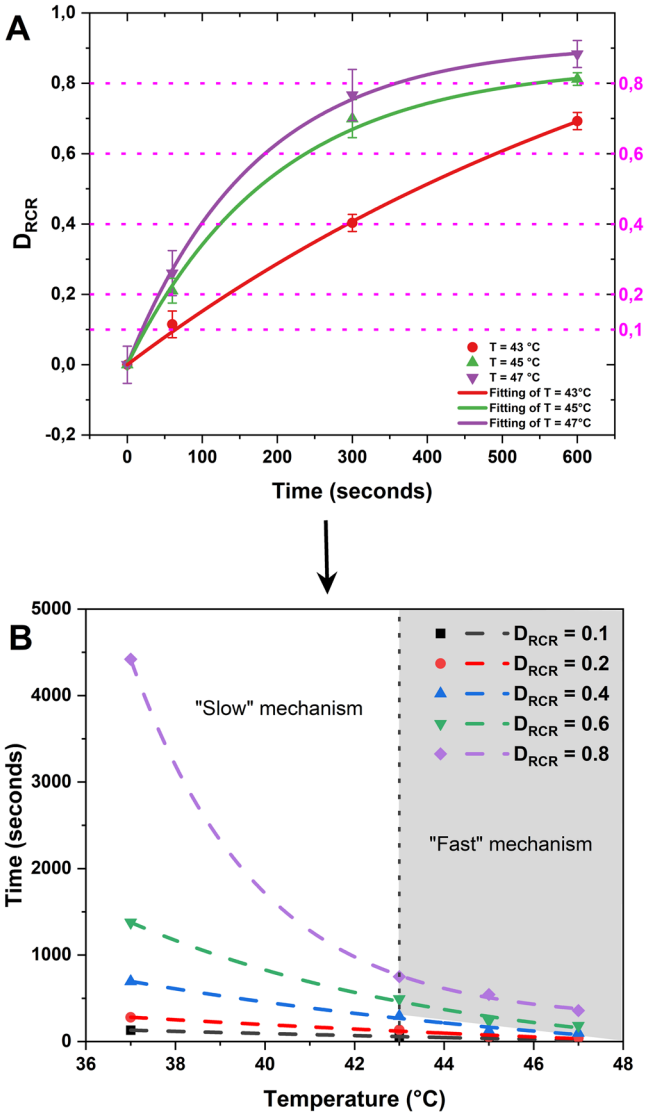

Figure 5. Time-temperature relationship analysis. (A) The same graph from Figure 4 is marked with reference lines (magenta dotted lines) for constructing isoeffect curves. (B) Isoeffect curves constructed from the reference lines presented in panel A. Each dashed curve represents a fixed damage, varying with time and temperature. The gray area represents the 'fast' mechanism.

A limitation of the present study is that respiration was assessed only in the NADH-linked pathway, without the use of $FADH_2$-linked substrates (e.g., succinate) to evaluate complex II–driven respiration. As complex I and complex II feed electrons independently into the ubiquinone pool, the current design does not allow us to determine whether the observed effects are specific to complex I (as demonstrated by Moreno-Loshuertos et al. (2023) [19]) or reflect a broader impairment of the electron transport chain. Although complex I contributes more substantially to the proton-motive force and ATP synthesis due to its proton-pumping activity [38], future experiments incorporating $FADH_2$-linked respiration, with or without inhibition of Complex II (e.g., malonate), and also inhibitors of the other ETC complexes would provide a more complete assessment of the sites and extent of thermal damage within the respiratory chain.

Incubation time had a clear and significant impact on the response of isolated mitochondria to thermal stress. At the shortest duration tested (1 min), temperature had no measurable effect on mitochondrial parameters, even at 47 °C, likely because this time frame only allowed the sample to reach thermal equilibrium, without sufficient time for damage to manifest. In contrast, more extended incubation periods resulted in temperature-dependent impairments in all assessed parameters, except for basal

respiration. This highlights the critical role of exposure duration in enabling thermal-induced mitochondrial dysfunction. It is also important to note that in the isolated system used here, mitochondria are directly exposed to experimental temperatures without the buffering effects of cellular structures. This increases their vulnerability and may amplify the observed thermal impact. Therefore, while isolated mitochondria offer precision and control for investigating bioenergetic mechanisms, they may not fully replicate the resilience of mitochondria in more complex biological systems. A logical and necessary next step would be to explore these thermally induced mitochondrial effects in more physiologically relevant models, such as intact cells or tissues. Such studies would provide a better understanding of how cellular environments modulate mitochondrial responses to heat and help reduce potential artifacts introduced by *in vitro* isolation. Beyond the direct mitochondrial effects observed *in vitro*, it is essential to recognize that, *in vivo*, mitochondrial dysfunction likely represents only part of the systemic metabolic disturbance caused by severe hyperthermia [39]. In the liver, where mitochondrial β-oxidation and the mitochondrial steps of gluconeogenesis are essential [40], such damage may suppress these pathways and favor extra-mitochondrial routes such as peroxisomal β-oxidation, which are less ATP-efficient and can alter redox and thermogenic balance [41].

A mathematical analysis was performed using RCR as a thermal damage parameter regarding the temperature-time relationship in the isolated mitochondria. In addition to serving as a parameter for assessing mitochondrial quality and efficiency [33], RCR demonstrated a consistent and reasonable temperature-time variation in our data, suggesting that it may be a reliable indicator for estimating thermal damage. The mathematical analysis of the isoeffect curves indicated that the temperature-time damage relationship consists of two mechanisms ('slow' and 'fast') which appear to have a temperature breakpoint at around 43 °C. This temperature is not surprising, as it falls within a range remarkably present in the literature. The relationship between temperature and time in hyperthermia of cells and tissues has been discussed since the 1980s [25,42,43]. Field and Morris (1983) and Field (1988) stated that the damage level in different cells *in vitro* or tissues *in situ* presents the same transition in the behavior in the range of 42–43 °C, even though there are differences in tissue sensitivities [25,42]. Field and Morris (1983) concluded that cells (*in vitro*) or tissues (*in situ*) were more resistant to heating rates when below 42 °C than above 43 °C, by a factor of four [42]. Sapareto and Dewey (1984) [44] even used 43 °C as a reference temperature to introduce the concept of 'cumulative equivalent minutes' (CEM) at 43 °C, which is a commonly used method for measuring the thermal dose in hyperthermia treatments for cancer therapy.

Frequently, the Arrhenius equation was used to describe the relationship between cell survival over time [45] or a range of temperatures [24]. However, the Arrhenius equation could not represent the survival curves between 43 and 55 °C, as pointed out by Pearce (2015) [45]. Roizin-Towle and Pirro (1991) [24] found a breakpoint temperature in the Arrhenius curves around 43.5 °C for human cells, and at 43 °C for rodent cells, indicating differences in thermotolerance rates when analyzing cells from different species. Additionally, the review by Lazlo (1992) [11] highlighted the effects of hyperthermia on cell structure and function, emphasizing that the consequences of heating above and below 42.5 °C differ significantly.

Concerning mitochondria, Willis et al. (2000) also found a breakpoint at the Arrhenius plot at 42 °C when mitochondria isolated from mouse liver were submitted to hyperthermia [20]. The 43 °C temperature was again reported as an essential threshold temperature in the most recent study regarding mitochondria, by Moreno-Loshuertos et al. (2023), who found degradation and inhibition of respiratory complexes and supercomplexes above this range [19]. Nevertheless, these mitochondria-driving studies do not consider the time parameter as relevant in their analyses. Our time evaluation, derived from the isoeffect curves obtained from isolated mitochondria, corroborates the findings of Field and Morris (1983) [42]. Our results indicated that time is more significant below 43 °C—referred to as a 'slow' mechanism—while its importance decreases above this threshold, where we identified a 'fast' mechanism. Consequently, these findings enhance our understanding of the temperature-time relationship in mitochondrial function. Furthermore, our mathematical approach offers a clearer insight into how this relationship operates, laying the basis for a future model that will describe this behavior in both physical and biological terms.

Lastly, in our study, we chose to use only one female mouse strain (C57BL/6J) around the same age (9–12 weeks), which are considered young adults, to minimize the variation factors between the results. Thus, aging, sex, tissue type, and genetic background may influence the generalizability of our findings.

Mitochondrial respiration and bioenergetic resilience decline with age, and aged mice display reduced respiratory capacity, lower membrane potential, diminished ATP production, and increased reactive oxygen species, which together would be expected to increase vulnerability to hyperthermic stress [46–48]. Additionally, strain- and substrain-dependent differences in mitochondrial function and stress responses have been consistently reported, such that baseline respiratory parameters, ROS production sites, and the magnitude of functional decline vary with genetic background [28,49]. For these reasons, the thermal thresholds and recovery dynamics described here for young adult female C57BL/6J mice liver may differ in aged animals, male mice, or in other strains and tissues.

5. Conclusion

This study investigated the effects of *in vitro* hyperthermia on mitochondrial function, focusing on the role of incubation time and temperature in driving thermal-induced damage. Our findings revealed that mitochondrial dysfunction is not only temperature-dependent but also critically influenced by the duration of exposure. While basal respiration remained relatively stable, significant impairments were observed in oxidative phosphorylation and electron transport chain efficiency, especially at prolonged incubation times and temperatures exceeding 43 °C. These results highlight the vulnerability of mitochondria under isolated conditions and underscore the necessity of incorporating both time and temperature into assessments of thermal stress.

Importantly, our mathematical analysis based on RCR values offered a novel way to interpret the temperature-time relationship through isoeffect curves. We identified a transition in the mechanism of damage around 43 °C—a threshold temperature repeatedly recognized in the literature. Below this point, damage accumulates gradually, suggesting ongoing repair or compensatory processes. Above it, damage occurs rapidly and, under our *in vitro* conditions, was not reversed during the measurement period, consistent with the onset of protein denaturation and failure of compensatory mechanisms. This 'slow-to-fast' transition aligns with previous observations and supports 43 °C as a critical benchmark in thermal biology.

Future research should aim to validate these findings in more physiologically relevant systems. Studying intact cells or tissue models will help clarify how intracellular organization and protective mechanisms modulate mitochondrial responses to heat. Additionally, the mathematical approach developed here could be refined and expanded into a predictive model, offering a quantitative framework to assess thermal risk and optimize protocols or experimental designs. Exploring how different cell types respond across this temperature-time matrix could also reveal species- or tissue-specific thermotolerance.

Acknowledgments

This manuscript is based on the PhD thesis of Natasha Ferreira Mezzacappo titled 'Effects of photobiomodulation, photodynamic therapy, and hyperthermia on mouse liver mitochondria bioenergetics,' submitted in 2024 to the São Carlos Institute of Physics, University of São Paulo. The authors acknowledge the use of OpenAI's ChatGPT (version 4.0) for improving the readability and grammatical correctness of the manuscript. The authors retain full responsibility for the content of this publication. All scientific content, interpretation, and conclusions remain the authors' sole responsibility.

Authors' contributions

Natasha F. Mezzacappo: conceptualization, methodology, validation, formal analysis, investigation, data curation, writing – original draft, writing – review & editing, visualization. Natalia M. Inada: conceptualization, methodology, validation, writing – original draft, writing – review & editing, visualization, supervision, project administration. José D. Vollet-Filho: formal analysis, visualization, writing – original draft, writing – review & editing. Michael L. Denton: writing—review & editing. Vladislav V. Yakovlev: writing—review & editing. Vanderlei S. Bagnato: conceptualization, methodology, resources, writing – original draft, visualization, supervision, project administration, funding acquisition.

Disclosure statement

The authors have no competing interests to declare that are relevant to the content of this article.

Data and materials availability

Data will be made available upon reasonable request.

Funding

This study was supported by São Paulo Research Foundation (FAPESP – grants number 2013/07276-1 and 2014/50857-8), by National Council for Scientific and Technological Development (CNPq – grant number 465360/2014-9), and by Coordination for the Improvement of Higher Education Personnel (CAPES – grant number 88887.511692/2020-00). The project was also partially funded by the U.S. Department of Defense through a Grant/Cooperative Agreement Award from the Air Force Office of Scientific Research (SOARD grant number FA9550-23-S-0001 and FA9550-23-1-0660).

ORCID

Natasha F. Mezzacappo http://orcid.org/0000-0002-9949-2580
Natalia M. Inada http://orcid.org/0000-0003-1940-186X
José D. Vollet-Filho http://orcid.org/0000-0002-9125-1694
Michael L. Denton http://orcid.org/0000-0003-3421-4085
Vladislav V. Yakovlev http://orcid.org/0000-0002-4557-1013
Vanderlei S. Bagnato http://orcid.org/0000-0003-4833-239X

References

[1] Desforges JF, Simon HB. Hyperthermia. N Engl J Med. 1993;329(7):483–487. doi: 10.1056/NEJM199308123290708.
[2] Roth J, Rummel C, Barth SW, et al. Molecular aspects of fever and hyperthermia. Neurol Clin. 2006;24(3):421–439. doi: 10.1016/j.ncl.2006.03.004.
[3] Kozłowski S, Brzezińska Z, Kruk B, et al. Exercise hyperthermia as a factor limiting physical performance: temperature effect on muscle metabolism. J Appl Physiol (1985). 1985;59(3):766–773. doi: 10.1152/jappl.1985.59.3.766.
[4] MacDougall JD, Reddan WG, Layton CR, et al. Effects of metabolic hyperthermia on performance during heavy prolonged exercise. J Appl Physiol. 1974;36(5):538–544. doi: 10.1152/jappl.1974.36.5.538.
[5] Wust P, Hildebrandt B, Sreenivasa G, et al. Hyperthermia in combined treatment of cancer. Lancet Oncol. 2002;3(8):487–497. doi: 10.1016/s1470-2045(02)00818-5.
[6] Hildebrandt B, Wust P, Ahlers O, et al. The cellular and molecular basis of hyperthermia. Crit Rev Oncol Hematol. 2002;43(1):33–56. doi: 10.1016/s1040-8428(01)00179-2.
[7] Park HG, Han SI, Oh SY, et al. Cellular responses to mild heat stress. Cell Mol Life Sci. 2005;62(1):10–23. doi: 10.1007/s00018-004-4208-7.
[8] Slimen IB, Najar T, Ghram A, et al. Reactive oxygen species, heat stress and oxidative-induced mitochondrial damage. A review. Int J Hyperthermia. 2014;30(7):513–523. doi: 10.3109/02656736.2014.971446.
[9] Cates J, Graham GC, Omattage N, et al. Sensing the heat stress by mammalian cells. BMC Biophys. 2011;4(1):16. doi: 10.1186/2046-1682-4-16.
[10] Baler R, Zou J, Voellmy R. Evidence for a role of Hsp 70 in the regulation of the heat shock response in mammalian cells. Cell Stress Chaper. 1996;1(1):33. doi: 10.1379/1466-1268(1996)001<0033:EFAROH>2.3.CO;2.
[11] Laszlo A. The effects of hyperthermia on mammalian cell structure and function. Cell Prolif. 1992;25(2):59–87. doi: 10.1111/j.1365-2184.1992.tb01482.x.
[12] Roti Roti JL. Cellular responses to hyperthermia (40–46° C): cell killing and molecular events. Int J Hyperthermia. 2008;24(1):3–15. doi: 10.1080/02656730701769841.
[13] Yatvin MB, Cramp WA. Role of cellular membranes in hyperthermia: some observations and theories reviewed. Int J Hyperthermia. 1993;9(2):165–185. doi: 10.3109/02656739309022533.
[14] Thomsen S, Pearce JA. Thermal damage and rate processes in biologic tissues. In: Optical-thermal response of laser-irradiated tissue. Dordrecht (Netherlands): Springer; 2011. p. 487–549.
[15] Clarke A, Pörtner HO. Temperature, metabolic power and the evolution of endothermy. Biol Rev Camb Philos Soc. 2010;85(4):703–727. doi: 10.1111/j.1469-185X.2010.00122.x.
[16] Macherel D, Haraux F, Guillou H, et al. The conundrum of hot mitochondria. Biochim Biophys Acta Bioenerg. 2021;1862(2):148348. doi: 10.1016/j.bbabio.2020.148348.
[17] Chrétien D, Bénit P, Ha H-H, et al. Mitochondria are physiologically maintained at close to 50 °C. PLoS Biol. 2018;16(1):e2003992. doi: 10.1371/journal.pbio.2003992.
[18] Lane N. Hot mitochondria? PLoS Biol. 2018;16(1):e2005113. doi: 10.1371/journal.pbio.2005113.

[19] Moreno-Loshuertos R, Marco-Brualla J, Meade P, et al. How hot can mitochondria be? Incubation at temperatures above 43 °C induces the degradation of respiratory complexes and supercomplexes in intact cells and isolated mitochondria. Mitochondrion. 2023;69:83–94. doi: 10.1016/j.mito.2023.02.002.
[20] Willis WT, Jackman MR, Bizeau ME, et al. Hyperthermia impairs liver mitochondrial function in vitro. Am J Physiol Regul Integr Comp Physiol. 2000;278(5):R1240–R1246. doi: 10.1152/ajpregu.2000.278.5.R1240.
[21] Šilkūnienė G, Žūkienė R, Naučienė Z, et al. Impact of gender and age on hyperthermia-induced changes in respiration of liver mitochondria. Medicina 2018. 2018;54:62.
[22] Žūkienė R, Naučienė Z, Šilkūnienė G, et al. Contribution of mitochondria to injury of hepatocytes and liver tissue by hyperthermia. Medicina (Kaunas). 2017;53(1):40–49. doi: 10.1016/j.medici.2017.01.001.
[23] Brooks G, Hittelman K, Faulkner J, et al. Temperature, skeletal muscle mitochondrial functions, and oxygen debt. Am J Physiol. 1971;220(4):1053–1059. doi: 10.1152/ajplegacy.1971.220.4.1053.
[24] Roizin-Towle L, Pirro JP. The response of human and rodent cells to hyperthermia. Int J Radiat Oncol Biol Phys. 1991;20(4):751–756. doi: 10.1016/0360-3016(91)90018-y.
[25] Field SB. The concept of thermal dose. Recent Results Cancer Res. 1988;107:1–6.
[26] Frezza C, Cipolat S, Scorrano L. Organelle isolation: functional mitochondria from mouse liver, muscle and cultured filroblasts. Nat Protoc. 2007;2(2):287–295. doi: 10.1038/nprot.2006.478.
[27] Fernández-Vizarra E, Ferrín G, Pérez-Martos A, et al. Isolation of mitochondria for biogenetical studies: an update. Mitochondrion. 2010;10(3):253–262. doi: 10.1016/j.mito.2009.12.148.
[28] Ronchi JA, Figueira TR, Ravagnani FG, et al. A spontaneous mutation in the nicotinamide nucleotide transhydrogenase gene of C57BL/6J mice results in mitochondrial redox abnormalities. Free Radic Biol Med. 2013;63:446–456. doi: 10.1016/j.freeradbiomed.2013.05.049.
[29] Kruger NJ. The bradford method for protein quantitation. In: Basic protein and peptide protocols. New Jersey: Humana Press; 2009. p. 9–16.
[30] Gnaiger E. Polarographic oxygen sensors, the oxygraph, and high-resolution respirometry to assess mitochondrial function. In: Drug-induced mitochondrial dysfunction. Hoboken, NJ, USA: Wiley; 2008. p. 325–352.
[31] Gnaiger E. Mitochondrial pathways and respiratory control: an introduction to OXPHOS analysis. Bioenerg Commun. 2020;2020:2.
[32] Coulson SZ, Duffy BM, Staples JF. Mitochondrial techniques for physiologists. Comp Biochem Physiol B Biochem Mol Biol. 2024;271:110947. doi: 10.1016/j.cbpb.2024.110947.
[33] Brand MD, Nicholls DG. Assessing mitochondrial dysfunction in cells. Biochem J. 2011;435(2):297–312. doi: 10.1042/BJ20110162.
[34] Logan SR. The origin and status of the Arrhenius equation. J Chem Educ. 1982;59(4):279. doi: 10.1021/ed059p279.
[35] Bischof JC, He X. Thermal stability of proteins. Ann NY Acad Sci. 2006;1066:12–33.
[36] Mazurenko S, Kunka A, Beerens K, et al. Exploration of protein unfolding by modelling calorimetry data from reheating. Sci Rep. 2017;7(1):16321. doi: 10.1038/s41598-017-16360-y.
[37] Christiansen EN, Kvamme E. Effects of thermal treatment on mitochondria of brain, liver and ascites cells. Acta Physiol Scand. 1969;76(4):472–484. doi: 10.1111/j.1748-1716.1969.tb04494.x.
[38] Wikström M, Pecorilla C, Sharma V. The mitochondrial respiratory chain. In: Enzymes. Academic Press; 2023. p. 15–36.
[39] Ding X, Gao B. Heat stress-mediated multi-organ injury: pathophysiology and treatment strategies. Compr Physiol. 2025;15(3):e70012. doi: 10.1002/cph4.70012.
[40] Rui L. Energy metabolism in the liver. Compr Physiol. 2014;4(1):177–197. doi: 10.1002/j.2040-4603.2014.tb00548.x.
[41] Cortassa S, Sollott SJ, Aon MA. Mitochondrial respiration and ROS emission during β-oxidation in the heart: an experimental-computational study. PLoS Comput Biol. 2017;13(6):e1005588. doi: 10.1371/journal.pcbi.1005588.
[42] Field SB, Morris CC. The relationship between heating time and temperature: its relevance to clinical hyperthermia. Radiother Oncol. 1983;1(2):179–186. doi: 10.1016/s0167-8140(83)80020-6.
[43] Gerner EW. Thermal dose and time-temperature factors for biological responses to heat shock. Int J Hyperthermia. 1987;3(4):319–327. doi: 10.3109/02656738709140402.
[44] Sapareto SA, Dewey WC. Thermal dose determination in cancer therapy. Int J Radiat Oncol Biol Phys. 1984;10(6):787–800. doi: 10.1016/0360-3016(84)90379-1.
[45] Pearce JA. Improving accuracy in Arrhenius models of cell death: adding a temperature-dependent time delay. J Biomech Eng. 2015;137(12):121006. doi: 10.1115/1.4031851.
[46] Sarver DC, Saqib M, Chen F, et al. Mitochondrial respiration atlas reveals differential changes in mitochondrial function across sex and age. Elife. 2024;13:RP96926. doi: 10.7554/eLife.96926.
[47] Torres AK, Jara C, Llanquinao J, et al. Mitochondrial bioenergetics, redox balance, and calcium homeostasis dysfunction with defective ultrastructure and quality control in the hippocampus of aged female C57BL/6J mice. Int J Mol Sci. 2023;24(6):5476. doi: 10.3390/ijms24065476.
[48] Haak JL, Buettner GR, Spitz DR, et al. Aging augments mitochondrial susceptibility to heat stress. Am J Physiol Regul Integr Comp Physiol. 2009;296:812–820.
[49] Mekada K, Yoshiki A. Substrains matter in phenotyping of C57BL/6 mice. Exp Anim. 2021;70(2):145–160. doi: 10.1538/expanim.20-0158.